

# MAGNETIC RESONANCE IN $Ti_mMg_nFe_{3-m-n}O_4$ FERRITES AND THEIR MAGNETIZATION\*

BY

Tanehiro NAKAU

(Received February 11, 1959)

## ABSTRACT

The ferromagnetic resonance absorption and the magnetization were measured on two natural single crystal samples of  $Ti_mMg_nFe_{3-m-n}O_4$  ferrites ( $m=0.51$ ,  $n=0.075$ , the Curie point= $125^\circ\text{C}$ ; and  $m=0.50$ ,  $n=0.072$ , the Curie point= $135^\circ\text{C}$ ), from room temperature to  $-195^\circ\text{C}$ . Each saturation magnetization obtained from magnetization measurement showed a broad maximum similar to those of Néel's P-type ferrites. The effective  $g$ -value and the magnetocrystalline anisotropy constant were obtained from resonance absorption experiments at the frequency of 25,700 Mc/sec. Each effective  $g$ -value showed a remarkable temperature dependence, corresponding to the above-mentioned feature of the magnetization. The magnetocrystalline anisotropy constant (first order anisotropy constant) changed with temperature in a somewhat similar manner to the magnetite, in agreement with the data on the magnetization. The anisotropy constant of one sample changed its sign at  $-155^\circ\text{C}$  and that of the other at  $-133^\circ\text{C}$ , and the direction of easy magnetization changed from the  $[111]$  to  $[100]$  direction with the decrease of temperature. These phenomena are discussed.

## 1. Introduction

Various investigations on ferromagnetic ferrites have been reported in recent years, and few ferrites (1~5) are known to show any low temperature transition of magnetocrystalline anisotropy or any remarkable temperature dependence of the  $g$ -value observed in microwave absorption experiment.

In the present paper are reported the results of microwave resonance absorption experiments and magnetization measurements on two natural single crystal samples of  $Ti_mMg_nFe_{3-m-n}O_4$  ferrites ( $m=0.51$ ,  $n=0.075$ , the Curie point= $125^\circ\text{C}$ ; and  $m=0.50$ ,  $n=0.072$ , the Curie point= $135^\circ\text{C}$ )\* of spinel type structure, as summarized in the following.

(1) Each first order anisotropy constant changed its sign at a certain low temperature, which might be a kind of low temperature transition.

---

\* Read before the annual meetings of the Physical Society of Japan, Oct., 19, 1957 and Oct., 16, 1958.

\*\* By spectral analysis, and other components such as Al, Cu, Mn and Si were negligible.

(2) The  $g$ -value obtained from the ferromagnetic resonance absorption experiment increased continuously with the decrease of temperature, between room temperature and the temperature at which the anisotropy constant changed its sign, thus showing a remarkable temperature dependence.

(3) A broad maximum of the saturation magnetization was observed at low temperatures\*. This is similar in peculiarity to the ferrites of the general formula:  $\text{Ni}_{1.5-a}\text{Mn}_a\text{FeTi}_{0.5}\text{O}_4$  ( $0.4 < a < 0.675$ ) known as Néel's P-type ferrites (6,7). The details of these features will be described in §3.

## 2. Experimental arrangement and samples

The method of measuring the resonance absorption was in principle the same as those (1,9) reported by many authors. The sample was mounted in a rectangular resonant cavity driven in the  $\text{TE}_{102}$  mode and connected with a wave guide magic T bridge. The microwave frequency used was about 25,700 Mc/sec. The external static magnetic field was applied normal to the wide face of the wave guide and orthogonal to the r-f magnetic field. The cavity was thermally insulated from the rest of the wave guide system. A thermocouple was soldered on the cavity, for measuring the temperature.

The samples were prepared as follows. The sample No. 1 was cut in the (110) plane from a single crystal specimen of the Curie point 125°C and shaped into an ellipse about 0.024 cm thick, of the major axis about 0.18 cm long and the minor axis about 0.11 cm. The sample No. 2 was cut in the (100) plane from a single crystal specimen of the Curie point 135°C, to be about 0.041 cm thick and of the major axis about 0.18 cm long and the minor axis about 0.013 cm. The X-ray investigation showed that, in the sample No. 1, the direction of the major axis coincided with the [110] direction of the crystal and the cut plane made an angle of 0.087 radians with the crystal plane (110). And in No. 2, the cut plane made an angle of 0.087 radians with the crystal plane (100) and the crystal axis [100] was in the sample plane, making an angle of 45° with the major axis. The errors of the value of the first order anisotropy constant due to neglecting these errors in the cut plane inclination did not exceed about 3%. The demagnetizing factors were calculated by the method of Osborn (10).

The field intensity was measured by using both a proton meter and a fluxmeter calibrated by it.

---

\* Read in part before the annual meeting of the Physical Society of Japan, Oct., 19, 1957. Recently, S. Akimoto, T. Katsura and M. Yoshida have reported that they found a particular mode of thermomagnetic curve similar to Néel's P-type ferrite with some specimens of synthetic polycrystals of titanomagnetites as solid solutions (reference 8).

A magnetic torsion balance (11) was used for the measurement of the magnetization\*.

### 3. Experimental results

#### a. Magnetic resonance

The first order anisotropy constant was observed to change its sign at a low temperature. The crystalline anisotropy constant  $K_1$  and the effective  $g$ -value were calculated from results of resonance absorption experiment by using the value of saturation magnetization obtained by the measurement of magnetization, while the second order anisotropy constant  $K_2$  was neglected, since it was sufficiently small as compared with  $K_1$  and was within the error of the experiment. The observation of resonance absorption was carried out continuously changing the temperature from the liquid nitrogen temperature to room temperature.

The absorption on a sample showed that the absorption was very broad near liquid nitrogen temperature, and especially in the  $[110]$  and  $[111]$  directions, the absorption changed according to both the intensity and the duration of the magnetic field previously applied to the sample. However, in the absorption of the sample which passed through such a process as follows, the above change almost disappeared and the measured results became steady and reproducible. Our results were obtained in this way.

The samples were cooled from room temperature to liquid nitrogen temperature in the magnetic field of 11,000~12,000 oersteds. After cooling, they were kept in the field of about 10,000 oersteds from liquid nitrogen temperature to a temperature about 40°C higher than the transition temperature of  $K_1$ \*\* (−110°C in the sample No. 1 and −100°C in the sample No. 2) except for the case when the field strength was decreased for the observation of resonance. Further, the resonance was observed with the field strength decreasing, because of the low permeability of the specimen. The analysis of results was limited from room temperature to a temperature near the transition temperature of  $K_1$ , since the resonance absorption became very broad and moreover a second order deformation of crystal structure might be expected below the transition temperature of  $K_1$ . The absorption was measured by observing the relative absorption, i.e. the change in the power  $P_r$ , reflected from the cavity on

---

\* The fused silica was used. The temperature was measured by a thermocouple set near the position of the sample. For the correction, the simultaneous measurements of the temperatures at this position and at the position of the sample were also carried out. The character of the magnetization measuring apparatus was tested to be good for the purpose by using a thin nickel plate of 0.004 cm thick.

\*\* The temperature at which  $K_1$  changes its sign is called the transition temperature of  $K_1$  in the following.

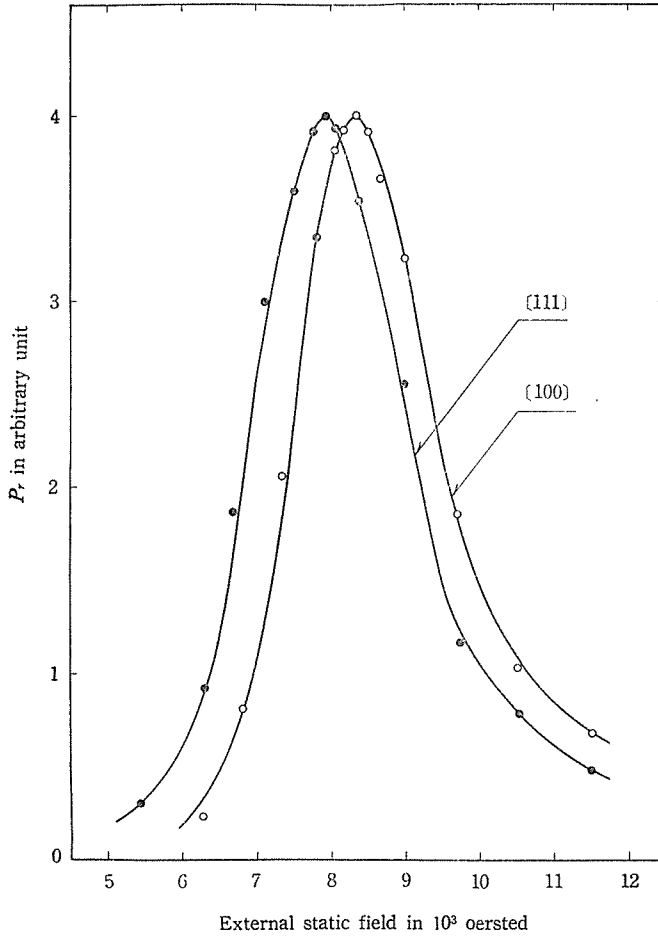


Fig. 1. Absorption curves of the sample No. 1 at room temperature.

resonance, with the incident power  $P_i$  maintained constant. It gives also qualitative information of the line breadth. The effective  $g$ -value and the value of  $K_1$  were calculated from the following expressions (1), (2a), (2b), (3a) and (3b) derived from the general formula (12) of resonance condition and corrected with respect to the inclination errors mentioned in § 2.

When a sample is an ellipsoidal ferromagnetic body whose principal axes are  $x$ ,  $y$ ,  $z$ -axes, the resonance angular frequency  $\omega$  in the case of cubic symmetry is given by

$$\omega = \gamma \left\{ [H_{\zeta} + (N_x \cos^2 \theta + N_z \sin^2 \theta - N_x \sin^2 \theta - N_z \cos^2 \theta + N_{\zeta}^0) M] \right. \\ \left. \times [H_{\zeta} + (N_y - N_x \sin^2 \theta - N_z \cos^2 \theta + N_{\zeta}^0) M] \right\}^{1/2} \quad (1)$$

under appropriate conditions. Here, the coordinate system  $(\xi, \eta, \zeta)$  is obtained by the rotation through the angle  $\theta$  round the  $y$ -axis ( $y \equiv \eta$ ), and  $H_\zeta$  is the external static magnetic field, the other quantities being usual ones (13, 14).

For a sample whose (100) plane is parallel to the  $(\xi\zeta)$  plane, by neglecting  $K_2$  which is small as compared with  $K_1$ ,  $N_\xi^e$  and  $N_\eta^e$  are given by

$$N_\xi^e = (K_1/M^2) \cos 4\phi, \quad (2a)$$

$$N_\eta^e = \left( \frac{3}{2} + \frac{1}{2} \cos 4\phi \right) K_1/M^2, \quad (2b)$$

where  $\phi$  is the angle between  $\zeta$ -axis and  $[100]$  direction. If the (110) plane is parallel to the  $(\xi\zeta)$  plane, we have

$$N_\xi^e = (2 - \sin^2\phi - 3 \sin^2 2\phi) K_1/M^2, \quad (3a)$$

and 
$$N_\eta^e = 2 \left( 1 - 2 \sin^2\phi - \frac{3}{8} \sin^2 2\phi \right) K_1/M^2. \quad (3b)$$

When the  $(\xi\zeta)$  plane makes a small angle with either of the (100) and (110) planes, the resonance condition differs from the expression (1).

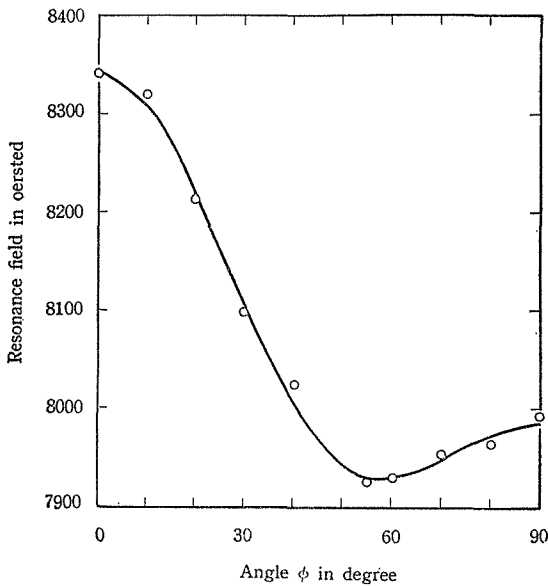


Fig. 2. Resonance field *versus* crystal orientation in the (110) plane of the sample No. 1 at room temperature.

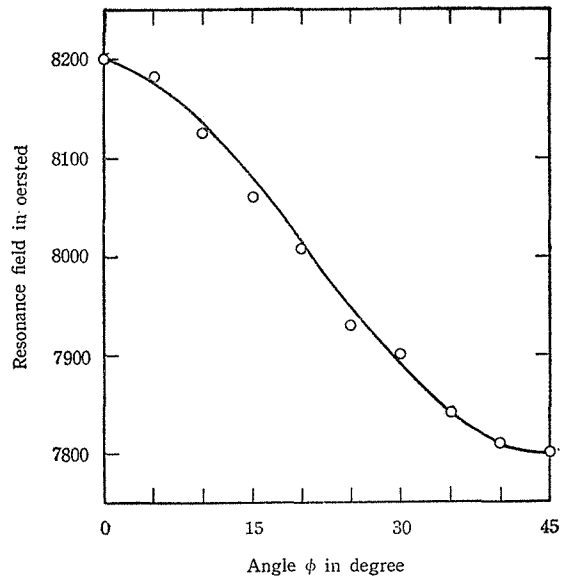


Fig. 3. Resonance field *versus* crystal orientation in the (100) plane of the sample No. 2 at room temperature.

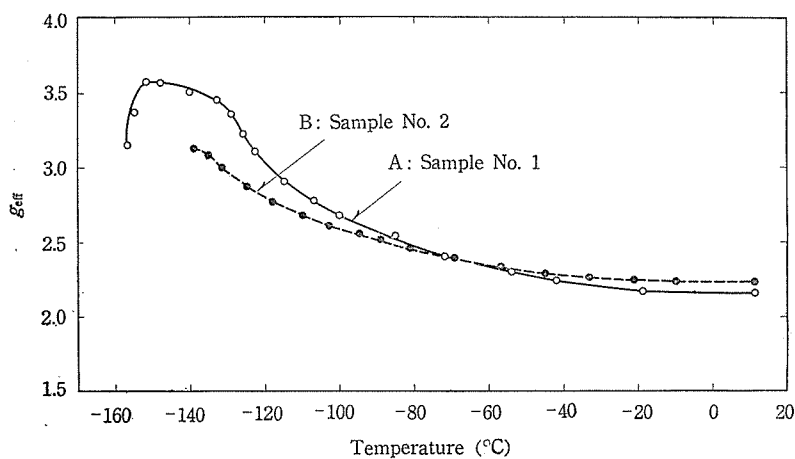
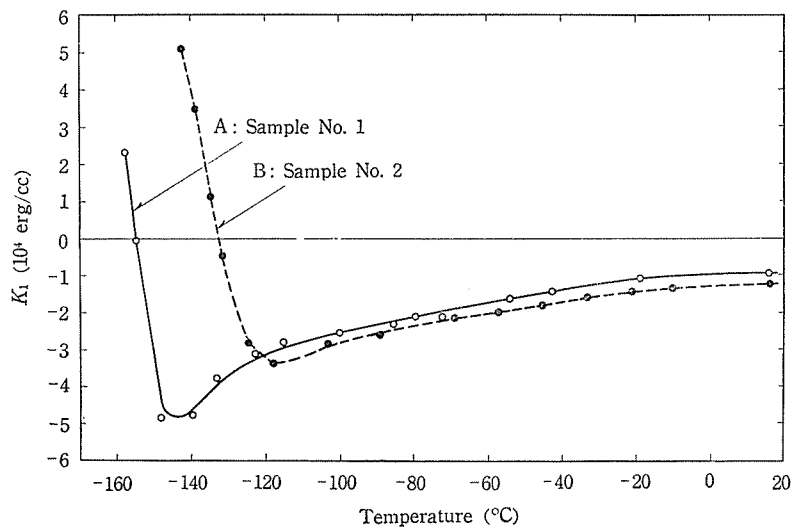
Fig. 4. Temperature dependence of effective  $g$ -value.Fig. 5. Temperature dependence of anisotropy constant  $K_1$ .

Table I.

Sample	$g_{\text{eff}}$	$K_1$
No. 1	$2.17 \pm 0.04$	$(-0.96 \pm 0.15) \times 10^4$ ergs/cc
No. 2	$2.23 \pm 0.04$	$(-1.26 \pm 0.19) \times 10^4$ ergs/cc

*The sample No. 1*

In this case, the sample was cut in the (110) plane. The magnetic absorption was observed mainly in the [100], [110] and [111] directions, applying the external static magnetic field parallel respectively to these directions and perpendicular to the r-f magnetic field parallel to the (110) plane.

Fig. 1 shows the relative absorption at room temperature in the [100] and [111] directions. Table I gives the average values of effective  $g$ -value and  $K_1$  at room temperature. Fig. 2 shows the resonance field at room temperature as a function of crystal orientation.  $\phi$  is the angle between the [100] direction and the external static field. The field strength at resonance decreased continuously with the decrease in temperature, so that the effective  $g$ -value became large at low temperature. This phenomenon is parallel to the change of magnetization *versus* temperature. The curve A in Fig. 4 represents the temperature dependence of the effective  $g$ -value calculated from the experimental results. The increasing tendency of the effective  $g$ -value becomes distinct around the temperature where the magnetization stops increasing (cf. Fig. 9). The curve A in Fig. 5 shows the value of  $K_1$  *versus* temperature, calculated from the experimental results. From this, it is recognized that the first order anisotropy constant changes its sign at about  $-155^\circ\text{C}$  and consequently the direction of easy magnetization changes.

With the decrease in temperature, the absorption became broad as shown in Figs. 1 and 6. This phenomenon corresponds to the decrease in permeability at low temperature. At about  $-160^\circ\text{C}$ , the absorption became very broad and the effective  $g$ -value showed the decreasing tendency also. These might be associated with a kind of low temperature transition.

The values of  $K_1$  and effective  $g$ -value are given in Table II.

Table II.

Temperature ( $^\circ\text{C}$ )	$g_{\text{eff}}$	$K_1$ ( $10^4$ ergs/cc)
-157	3.15	+2.05
-155	3.37	-0.03
-148	3.57	-4.94
-140	3.50	-4.75
-133	3.45	-3.73
-123	3.10	-3.12
-115	2.91	-2.86
-100	2.67	-2.58
-85	2.53	-2.37
-79	2.41	-2.07
-72	2.40	-2.11
-54	2.29	-1.61
-42	2.24	-1.47
-19	2.17	-1.08

*The sample No. 2*

The sample No. 2 was cut in the (100) plane. Magnetic absorption was observed mainly in the [100] and [110] directions and the direction making an angle of  $15^\circ$  with the [100] direction in the (100) plane.

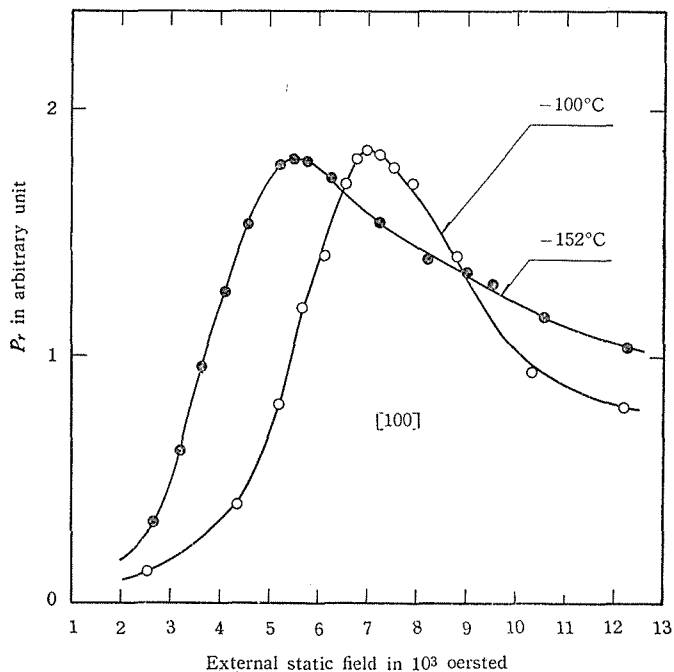


Fig. 6. Absorption curves in the  $[100]$  direction of the sample No. 1 at  $-152^{\circ}\text{C}$  and  $-100^{\circ}\text{C}$ .

In this case, the external static magnetic field was applied parallel to the  $(100)$  plane and normal to the r-f magnetic field parallel to the  $(100)$  plane.

The experimental results were essentially the same as those with the sample No. 1. The temperature dependence of the effective  $g$ -value was similar to that of the sample No. 1, and the first order anisotropy constant  $K_1$  changed its sign at a low temperature as in the sample No. 1.

Fig. 3 shows the experimental value of the resonance field as a function of the crystal orientation.  $\phi$  is the angle between the external static magnetic field and the  $[100]$  direction. The effective  $g$ -value is plotted as a function of temperature in the curve B of Fig. 4. The curve B in Fig. 5 gives the value of  $K_1$  as a function of temperature, showing that  $K_1$  changes its sign at about  $-133^{\circ}\text{C}$ . The increasing tendency of  $K_1$  is remarkable in the figure at temperatures near the transition temperature of  $K_1$ , but the curve becomes flat at lower temperatures, under the assumption that the crystal is still cubic below  $-152^{\circ}\text{C}$ , though the value of  $K_1$  was not plotted for the reason mentioned above.

The value of  $K_1$  and the effective  $g$ -value are listed in Tables I and III.

The results obtained from the resonance absorption experiment on the sample



No. 2 agreed with those on the sample No. 1 in main features. In the sample No. 2, the temperature at which an anomaly starts in the resonance broadness and the decrease of effective  $g$ -value was by about  $15^\circ\text{C}$  lower than the transition temperature of  $K_1$ , while in the sample No. 1, the corresponding temperature almost agreed with the transition temperature of  $K_1$ , thus the anomaly temperatures of the two samples being near together. This difference may be induced by any difference in condition of crystallization, though contents of their main components are not the same.

Table III.

Temperature ( $^\circ\text{C}$ )	$g_{\text{eff}}$	$K_1$ ( $10^4$ ergs/cc)
-142	3.04	+5.12
-139	3.12	+3.48
-135	3.09	+1.14
-132	3.00	-0.48
-125	2.86	-2.79
-118	2.77	-3.38
-103	2.60	-2.86
-89	2.51	-2.59
-69	2.40	-2.20
-57	2.34	-2.01
-45	2.29	-1.82
-33	2.26	-1.62
-21	2.24	-1.46
-10	2.23	-1.33

#### b. Magnetization

The experimental results of measurement of magnetization showed a fall of magnetization and a change in the direction of easy magnetization at low temperatures. It was studied whether the feature of the fall of magnetization is the same as that displayed by magnetite (15, 16, 17) or not. We observed the warming curve of magnetization in various fields and the magnetization curve after cooling in strong field as well as in zero field. The result showed that the fall of magnetization at low temperatures was not similar to that of magnetite but similar to that of Néel's P-type ferrite; namely the curve of saturation magnetization *versus* temperature showed a broad maximum. This property corresponds to the increasing tendency of the effective  $g$ -value in the resonance absorption at low temperatures. The experimental results are described in the following.

#### The sample No. 1

The magnetization curves in Fig. 7 show that the direction of easy magnetization changes from the  $[111]$  to  $[100]$  direction at low temperatures\*. The value of the anisotropy constant  $K_1$  was calculated by using results of the resonance absorption at temperatures near and above the transition temperature of  $K_1$ . However,  $K_1$  was calculated from the difference between the energies required for magnetization obtained from the magnetization curves. The value was of the order of  $10^5$  erg/cc at  $-180^\circ\text{C}$ , on the assumption that the crystal has a cubic symmetry.

\* A simple observation was made for ascertaining the change of the direction of easy magnetization: a sample placed in magnetic field rotated at low temperatures with temperature decrease, which corresponds to the change of the direction of easy magnetization.

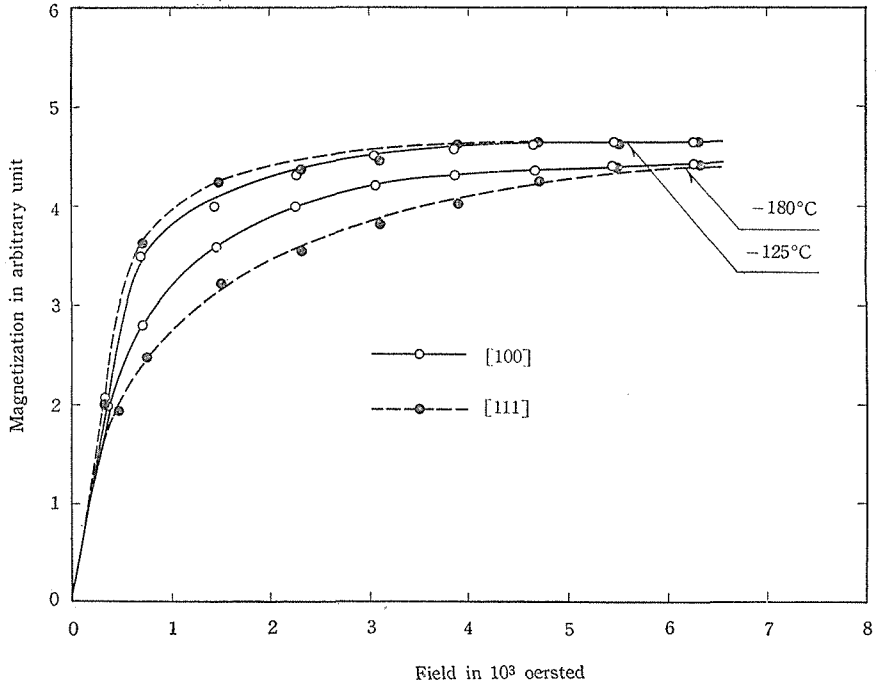


Fig. 7. Magnetization curves in the [100] and [111] directions of the sample No. 1.

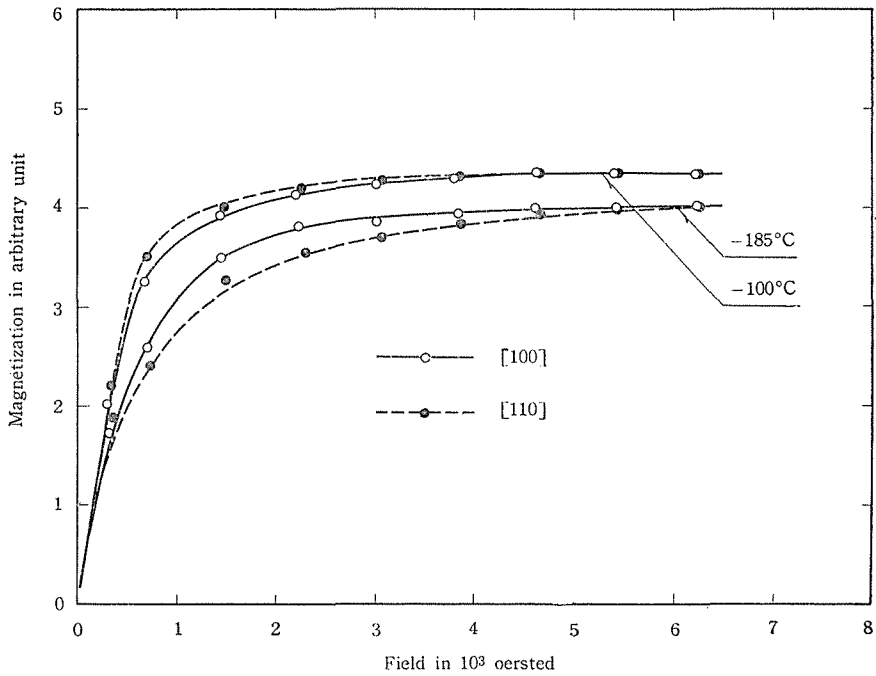


Fig. 8. Magnetization curves in the [100] and [110] directions of the sample No. 2.

The saturation magnetization was determined by using a nickel plate\* as the standard. The value of saturation magnetization\*\* at room temperature was 95 cgs. The curve A in Fig. 9 represents a temperature dependence of magnetization in the  $[100]$  direction of the sample No. 1. This is a warming curve in which the value of magnetization was measured in the field of 8,000 oersteds after cooling in the field of 11,000 oersteds in the  $[100]$  direction from room temperature to liquid nitrogen temperature. This curve can be regarded to show the curve of saturation magnetization *versus* temperature as shown in the discussion later. The curve A in Fig. 10 shows a warming curve of magnetization in the  $[111]$  direction in the field of 7,200 oersteds. From these results, it can be supposed that the values of magnetization

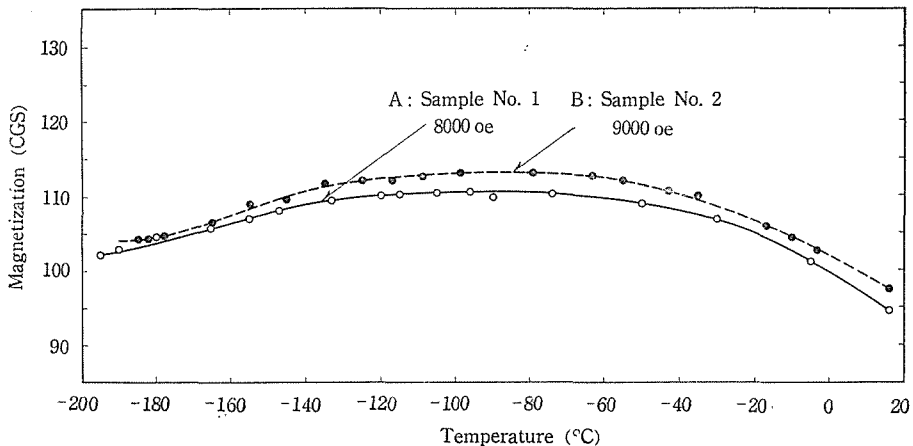


Fig. 9. Warming curves in the  $[100]$  direction of the samples No. 1 and No. 2 after cooling in field of 11,000 oersteds parallel to  $[100]$ .

in various directions of the crystal almost coincide with each other in such strong fields, in spite of the influence of crystalline anisotropy, etc. The magnetization curves in Fig. 11 were obtained after cooling from room temperature to liquid nitrogen temperature in the field of 11,000 oersteds in the  $[100]$  direction. The values at  $-190^\circ\text{C}$  were obtained by decreasing the field strength and the values at  $-180^\circ\text{C}$  by increasing the field strength from zero. In either case, the magnetization took the nearly saturated value in the field of about 3,000 oersteds. Therefore, it is reasonable to regard the fall of magnetization as that of the saturation magnetization. Besides, by considering the magnetization curves in Figs. 7 and 11, it is concluded that the magnetization in Fig. 9 represents the value of saturation magnetization.

\* The nickel content being 99.6%.

\*\* From this measurement, the value per gramme is known, and the value per unit volume is calculated, using the density determined from lattice constant of pure titanomagnetite, since the error seems to be within about 1% (reference 18).

The temperature dependence of saturation moment (per gramme) is represented by a smooth curve as shown in Fig. 13, so the crystal is evidently of sufficiently stable single phase (18, 19, 20).

*The sample No. 2*

The magnetization was observed in the  $[100]$  and  $[110]$  directions. The magnetization curves in Fig. 8 show that the direction of easy magnetization changes as in the sample No. 1. The energy difference obtained from the magnetization curves gives also the value of the order of  $10^5$  erg/cc at  $-185^\circ\text{C}$ , on the same assumption as with the sample No. 1.

The value of saturation magnetization at room temperature was 98 cgs. A warming curve of the magnetization in the  $[100]$  direction is shown in Fig. 9. The value of magnetization was obtained in the field of 9,000 oersteds after cooling in the field of 11,000 oersteds in the  $[100]$  direction. The temperature at which the magnetization begins to fall is higher than that of the sample No. 1. A warming curve of magnetization in the  $[110]$  direction is shown in Fig. 10. From the curves in Fig. 8 and the magnetization curve in Fig. 12 which was obtained after cooling in the field of 6,400 oersteds, it is evident that the curve B in Fig. 9 shows that of saturation magnetization versus temperature. The temperature dependence of saturation moment is also quite similar to that of the sample No. 1. Thus the features of the sample No. 2 are essentially the same as those of the sample No. 1.

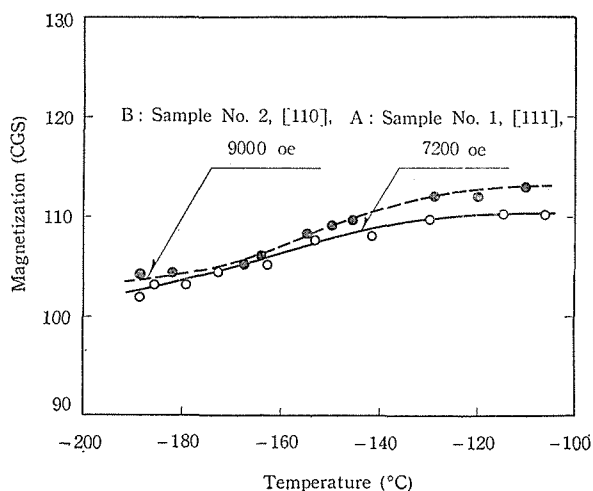


Fig. 10. Warming curves in the  $[111]$  direction of the sample No. 1 and in the  $[110]$  direction of the sample No. 2.

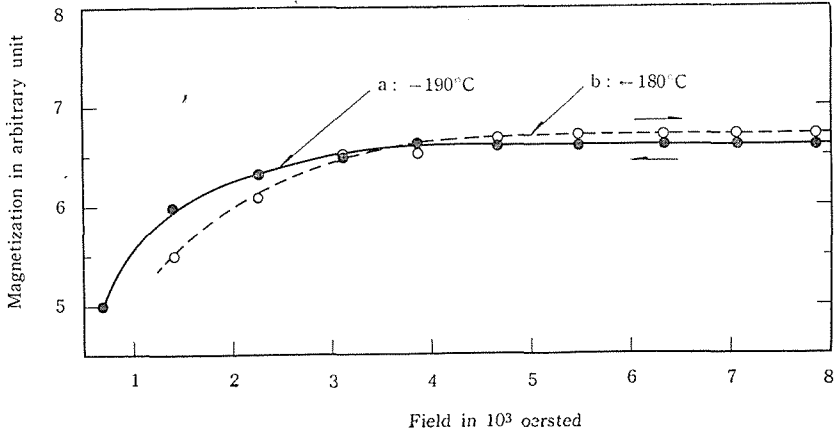


Fig. 11. Magnetization curves in the  $[100]$  direction of the sample No. 1 at  $-190^\circ\text{C}$  and  $-180^\circ\text{C}$  after cooling in the field of 11,000 oersteds parallel to  $[100]$ .

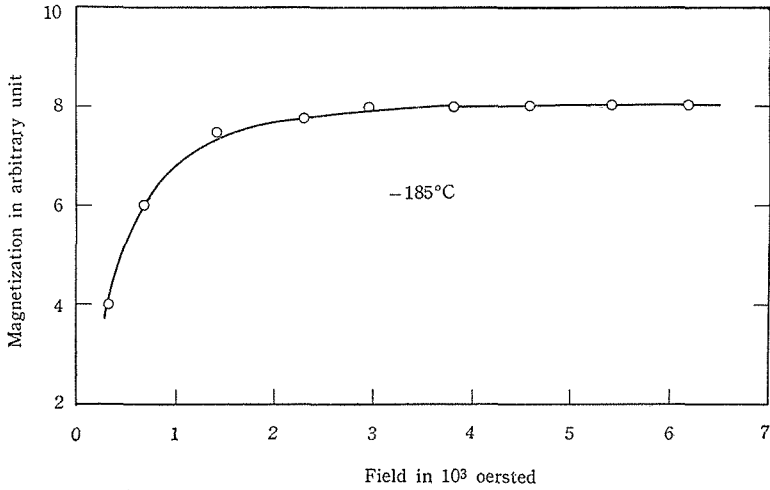


Fig. 12. Magnetization curve in the  $[100]$  direction of the sample No. 2 at  $-185^\circ\text{C}$  after cooling in the field of 6,400 oersteds parallel to  $[100]$ .

#### 4. Discussion of results

The structure of the specimens is of spinel type, and their direction of easy magnetization changed from the  $[111]$  to  $[100]$  direction as shown in Fig. 5, in accordance with the results of measurement of magnetization. This phenomenon is somewhat similar to that of magnetite. In magnetite, the data by Bickford (1) show that the transition temperature of the crystalline anisotropy is by about  $12^\circ\text{C}$  lower than the temperature at which the first order anisotropy constant changes its sign.

Besides, a sudden fall of the magnetization and the other anomalies are observed around the transition temperature (15, 16, 17, 21, 22). In the present specimens, however, such a clear sudden fall as observed in magnetite could not be found, though an anomaly in magnetic resonance absorption was observed as described in §3. The phenomena in magnetite are related to the ordered arrangement of ferrous and ferric ions in octahedral lattice sites (21, 23). But it is not accepted that such a mechanism might contribute to interpreting the phenomena in the present case, since plausibly  $\text{Fe}^{3+}$  ions as a small content of metal ions and  $\text{Fe}^{2+}$  ions as a large content exist together in octahedral lattice sites. Then, titanium ions might play an important role in the present phenomena from a structural point of view.

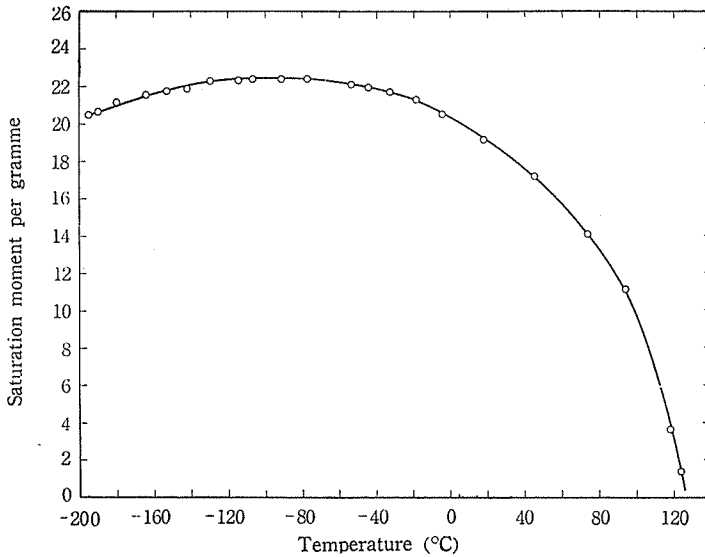


Fig. 13. Saturation magnetization *versus* temperature of the sample No. 1.

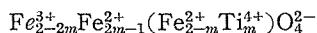
We try an explanation for the increase of effective  $g$ -value with the decrease of temperature by using the formula derived by Wangsness (24) and others (6, 25). Now, at 0°K, the effective  $g$ -value is given by

$$g_{\text{eff}} = (\sum g_{A_i} S_{A_i} - \sum g_{B_i} S_{B_i}) / (\sum S_{A_i} - \sum S_{B_i}), \quad (4)$$

where  $S_{A_i}$  and  $S_{B_i}$  are respectively the resultant electron spin quantum numbers of an individual ion in A sites (tetrahedral sites) and B sites (octahedral sites). In order to evaluate  $g_{\text{eff}}$  as a function of temperature,  $S_{A_i}$  and  $S_{B_i}$  in (4) are replaced by  $S_{A_i} B_{A_i}$  and  $S_{B_i} B_{B_i}$ , where  $B_{A_i}$ ,  $B_{B_i}$  are Brillouin functions.

Then, for simplifying the problem, we consider titanomagnetites, where the configuration of titanium ions governs the magnetization, though magnesium ions of

small content might play a particular role. If the  $Ti^{4+}$  ions are assumed to occupy always B sites, for  $m \geq 0.5$  the configuration of  $Ti_mFe_{3-m}O_4$  can be given by



with the saturation moment  $(2-2m)\mu_B$ , (26, 27)

where the ions in the bracket occupy B sites. As Néel (26) pointed out, however, the experimental facts are not sufficiently existing to support this formula.

A calculation of  $g_{\text{eff}}$  using  $Ti_{0.5}Fe_{2.5}O_4$  as an approximation is carried out on the assumption that the configuration is represented by the above formula. Now,  $Fe^{3+}$  ions occupy A sites only and  $Fe^{2+}$  ions B sites only. The atomic ground state of  $Fe^{3+}$  ion is  ${}^6S$  and that of  $Fe^{2+}$  ion  ${}^5D$ . So it is reasonable that  $g_A$  is 2. When  $g_B$  is 2.2,  $g_{\text{eff}}$  becomes 3.2 from (4), because  $S_A$  is 5/2 and  $S_B$  is 2. If the effective  $g$ -value at the temperature at which  $K_1$  changes its sign is equal to that at 0°K, this value almost agrees with the experimental value of the sample No. 2. A trial calculation of  $g_{\text{eff}}$  and the magnetization as functions of temperature for  $Ti_{0.5}Fe_{2.5}O_4$  was carried out by using the above values of  $g$ 's and Brillouin functions in the case of  $S_A=5/2$  and  $S_B=2$ , adjusting the parameters such that the effective  $g$ -value and the magnetization take the values near the experimental values. It could explain qualitatively the experimental results. However, since the formula for  $g_{\text{eff}}$  is an approximate one and the parameters mentioned above are obtained by the measurement of susceptibility at high temperatures (7), we will not go further into the discussion of  $g_{\text{eff}}$ . The decrease of the effective  $g$ -value may be another problem considering it as an anomaly.

From the above-mentioned formula, the saturation moment at 0°K is evaluated by assuming the formula  $[Ti_lFe_{3-l}O_4]_{1-n}[MgFe_2O_4]_n$  for  $Ti_mMg_nFe_{3-m-n}O_4$ . If  $[MgFe_2O_4]$  has the formula  $[Fe^{3+}(Mg^{2+}Fe^{3+})O_4^{2-}]$ , the calculated saturation moment at 0°K is  $0.83 \mu_B$  for the specimen No. 1 and  $0.86 \mu_B$  for the specimen No. 2. These values show good agreement with the values  $0.81 \mu_B$  and  $0.83 \mu_B$  for the specimens No. 1 and No. 2 at 0°K respectively as estimated from the curves in Fig. 9.

Toe broadness of the absorption is evidently related to the low permeability, though it may also be due to other causes.

For a more exact explanation of the above phenomena, we need other measurements at low temperatures, i.e., measurements of electrical conductivities, specific heat and etc., and also X-ray study at low temperatures.

### Acknowledgments

The author wishes to thank cordially Professor I. Takahashi for his kind guidance. He is also indebted to Professor N. Kumagai, Dr. N. Kawai and Mr. S. Kume for the

use of their equipment and for their help, and to Mr. T. Seto for his X-ray analysis, to Mr. S. Okasaki of Matsushita Elec. Co. for his spectral analysis, and to Dr. K. Yoshida for his useful discussions.

## REFERENCES

1. L. R. BICKFORD, *Phys. Rev.*, **78** (1950), 449.
2. D. W. HEALEY, *Phys. Rev.*, **86** (1952), 1009.
3. W. A. YAGER, J. K. GALT and F. R. MERRIT, *Phys. Rev.*, **99** (1955), 1203.
4. T. OKAMURA, Y. TORIZUKA and Y. KOJIMA, *Phys. Rev.*, **84** (1951), 372.
5. T. R. MCGUIRE, *Phys. Rev.*, **97** (1955), 831.
6. E. W. GORTER, *Philips Res. Rep.*, **9** (1954), 295, 321, 403.
7. L. NÉEL, *Ann. Phys.*, **3** (1948), 137.
8. S. AKIMOTO, T. KATSURA and M. YOSHIDA, *J. Geomag. Geoelect.*, **9** (1957), 165.
9. R. D. ARNOLD and A. F. KIP, *Phys. Rev.*, **75** (1949), 1199.
10. J. A. OSBORN, *Phys. Rev.*, **67** (1945), 351.
11. N. KAWAI, Report International Congress, Mexico (1956).
12. J. SMIT and H. G. BELJERS, *Philips Res. Rep.*, **10** (1955), 113; H. SUHL, *Phys. Rev.*, **97** (1955), 555.
13. C. KITTEL, *Phys. Rev.*, **73** (1948), 155.
14. C. KITTEL, *Phys. Rev.*, **76** (1949), 743.
15. P. WEISS and R. FORRER, *Ann. Phys.*, [10] **12** (1929), 279.
16. C. A. DOMENICALLI, *Phys. Rev.*, **78** (1950), 458.
17. B. A. CALHOUN, *Phys. Rev.*, **94** (1954), 1577.
18. N. KUMAGAI, N. KAWAI and S. KUME, *Memo. Coll. Sci. Univ. Kyoto*, **21** (1954), 287.
19. N. KAWAI, S. KUME and S. SASAJIMA, *Proc. Japan Acad.*, **30** (1954), 588.
20. N. KAWAI, *Proc. Japan Acad.*, **31** (1955), 346.
21. E. J. W. VERWEY, *Nature* **144** (1939), 327; E. J. W. VERWEY and P. W. HAAYMAN, *Physica* **8** (1941), 979.
22. S. C. ABRAHAMS and B. A. CALHOUN, *Acta. Cryst.*, **6** (1953), 105.
23. C. G. SHULL, *Colloque International de Magnétisme de Grenoble*, (1958).
24. R. K. WANGSNESS, *Phys. Rev.*, **91** (1953), 1085.
25. N. TSUYA, *Prog. Theor. Phys.*, **7** (1952), 263.
26. L. NÉEL, *Advanc. Phys.*, **4** (1955), 191.
27. E. W. GORTER, *Advanc. Phys.*, **6** (1957), 336.